

## Shock wave studies of the reactions $\text{HO} + \text{H}_2\text{O}_2 \rightarrow \text{H}_2\text{O} + \text{HO}_2$ and $\text{HO} + \text{HO}_2 \rightarrow \text{H}_2\text{O} + \text{O}_2$ between 930 and 1680 K

H. Hippler, H. Neunaber, and J. Troe

Citation: *The Journal of Chemical Physics* **103**, 3510 (1995); doi: 10.1063/1.470235

View online: <http://dx.doi.org/10.1063/1.470235>

View Table of Contents: <http://scitation.aip.org/content/aip/journal/jcp/103/9?ver=pdfcov>

Published by the AIP Publishing

### Articles you may be interested in

Theoretical characterization of the potential energy surface for  $\text{H} + \text{O}_2 = \text{HO}^* + \text{O} = \text{OH} + \text{O}$ . III. Computed points to define a global potential energy surface

*J. Chem. Phys.* **94**, 7068 (1991); 10.1063/1.460240

Shock wave study of the reaction  $\text{HO}_2 + \text{HO}_2 \rightarrow \text{H}_2\text{O}_2 + \text{O}_2$  : Confirmation of a rate constant minimum near 700 K

*J. Chem. Phys.* **93**, 1755 (1990); 10.1063/1.459102

Studies of reactions of importance in the stratosphere. III. Rate constant and products of the reaction between ClO and HO<sub>2</sub> radicals at 298 K

*J. Chem. Phys.* **72**, 2364 (1980); 10.1063/1.439484

Kinetic Studies of Hydroxyl Radicals in Shock Waves. V. Recombination via the  $\text{H} + \text{O}_2 + \text{M} \rightarrow \text{HO}_2 + \text{M}$  Reaction in Lean Hydrogen—Oxygen Mixtures

*J. Chem. Phys.* **43**, 3237 (1965); 10.1063/1.1697298

SinglePulse Shock Tube Studies of the Kinetics of the Reaction  $\text{N}_2 + \text{O}_2 \rightarrow 2\text{NO}$  between 2000–3000°K

*J. Chem. Phys.* **27**, 850 (1957); 10.1063/1.1743864



# Shock wave studies of the reactions $\text{HO} + \text{H}_2\text{O}_2 \rightarrow \text{H}_2\text{O} + \text{HO}_2$ and $\text{HO} + \text{HO}_2 \rightarrow \text{H}_2\text{O} + \text{O}_2$ between 930 and 1680 K

H. Hippler

*Institut für Physikalische Chemie und Elektrochemie, Universität Karlsruhe, Kaiserstrasse 12, D-76128 Karlsruhe, Germany*

H. Neunaber and J. Troe

*Institut für Physikalische Chemie, Universität Göttingen, Tammannstrasse 6, D-37077 Göttingen, Germany*

(Received 29 December 1994; accepted 31 May 1995)

Monitoring resonance absorption at the  $Q_1(4)$  line near 308.4 nm, HO concentration-time profiles were recorded during the thermal decomposition of  $\text{H}_2\text{O}_2$  in shock waves between 930 and 1680 K. The results were analyzed with respect to the reactions  $\text{HO} + \text{H}_2\text{O}_2 \rightarrow \text{H}_2\text{O} + \text{HO}_2$  (2) and  $\text{HO} + \text{HO}_2 \rightarrow \text{H}_2\text{O} + \text{O}_2$  (3). Above 800 K, reaction (2) shows a strong increase of the rate constant with temperature. Over the range  $240 \leq T \leq 1700$  K the apparent rate constant is represented as  $k_2 = [1.7 \cdot 10^{18} \cdot \exp(-14\,800 \text{ K}/T) + 2.0 \cdot 10^{12} \exp(-215 \text{ K}/T)] \text{ cm}^3 \text{ mol}^{-1} \text{ s}^{-1}$ . The rate constant  $k_3$  decreases from a value of  $2.0 \cdot 10^{13}$  at 1100 K to a minimum value of  $1.1 \cdot 10^{13}$  at 1250 K, and rises again to a value of  $4.5 \cdot 10^{13} \text{ cm}^3 \text{ mol}^{-1} \text{ s}^{-1}$  at 1600 K. The anomalous temperature dependences of  $k_2$  and  $k_3$  suggest mechanisms involving intermediate complex formation. © 1995 American Institute of Physics.

## I. INTRODUCTION

Because of their relevance to hydrogen and hydrocarbon oxidation in atmospheric chemistry and in combustion, the reactions



and



have received considerable attention.<sup>1,2</sup> Near room temperature, a consistent set of data exists. Between 500 and 800 K, less information is available whereas at temperatures above 1000 K only few and controversial results have been reported. In previous work<sup>3-7</sup> we have investigated reactions (2) and (3) as secondary processes of the shock wave induced thermal dissociation of  $\text{H}_2\text{O}_2$ ,



In the lower part of the investigated temperature range 800–1100 K, reactions (1) and (2) and the subsequent self-reaction of  $\text{HO}_2$  radicals



dominate whereas in the upper part also reaction (3) plays an important role. The simplicity of the mechanism and the possibility to monitor the concentrations of several species allow for a separate determination of all four rate constants  $k_1 - k_4$ .

In our previous work we used uv absorption spectroscopy of  $\text{H}_2\text{O}_2$  and  $\text{HO}_2$  for detection. With this technique,  $k_1$  and  $k_4$  could be determined reliably, while data on  $k_2$  and  $k_3$  were more difficult to obtain. Nevertheless, our analysis<sup>3</sup> of  $\text{HO}_2$  yields in the dissociation of  $\text{H}_2\text{O}_2$  indicated a dramatic change of the temperature coefficient of reaction (2) near 800 K. While the apparent activation energy and the preexponential factor of  $k_2$  were low at  $T < 800$  K, a change to much larger activation energy and anomalously high preexponen-

tial factor was observed at  $T > 800$  K. Using ring laser line absorption measurements of HO concentrations, a new and more sensitive access to the rate constants  $k_2$  and  $k_3$  became available such as indicated by our preliminary measurements near 1000 K.<sup>7</sup> It was the aim of the present work to extend these measurements and to confirm the earlier conclusions about an unusual temperature dependence of  $k_2$ . Likewise more extensive measurements on the important reaction (3) had to be performed, since the  $\text{H}_2\text{O}_2$  decomposition system provides the most direct access to  $k_1 - k_4$  under high temperature conditions.

Our measurements of the temperature coefficients of reactions (2)–(4) led to quite differing behavior: While reaction (2) showed a change from a weakly to strongly positive temperature coefficient near 800 K, reaction (4) is characterized by a deep rate constant minimum near to the same temperature. On the other hand, reaction (3) shows a rate constant minimum near 1250 K. One may speculate on the origin of these interesting properties and tentatively attribute the results to the formation of  $\text{H}_3\text{O}_3$ ,  $\text{H}_2\text{O}_3$ , and  $\text{H}_2\text{O}_4$  intermediate complexes in reactions (2)–(4), respectively. Without *ab initio* calculations of reliable potential energy surfaces, detailed conclusions about the participation of such complexes cannot be drawn.<sup>8</sup> However, the present measurements provide considerable experimental material for an interpretation in terms of an intermediate complex mechanism, see below.

## II. EXPERIMENTAL TECHNIQUE

The thermal decomposition of  $\text{H}_2\text{O}_2$  in the present work was studied in incident and reflected shock waves over the temperature range 930–1680 K.  $\text{H}_2\text{O}_2$  concentrations of 1–1000 ppm in Ar and total gas concentrations of  $(2-8) \cdot 10^{-6} \text{ mol cm}^{-3}$  were employed. The shock waves were generated in an aluminum shock tube of 20 cm inner diameter and a 7 m test section. For more details of our

experimental setup, see Ref. 7. HO radicals were monitored by resonance absorption at the  $Q_1(4)$  line at 308.4172 nm (wavelength in air). The radiation from an Ar-ion laser pumped cw-ring dye laser (Coherent CR-899-21) with intra-cavity frequency doubling served as light source. The light beam was split into an analysis beam and a reference beam. The absorption was determined with two photodiode detectors. Absorption-time profiles were converted into concentration-time profiles using Beer's law. The relevant absorption cross sections  $\sigma(T, p)$  were calculated using oscillator strengths and additional parameters from Refs. 9 and 10. For the  $Q_1(4)$ -line, the results between 1000 and 2500 K can be represented (within 15% accuracy) by the expressions

$$\sigma/\text{cm}^2 = 4.17 \cdot 10^{-16} - 3.89 \cdot 10^{-19}T + 1.48 \cdot 10^{-22}T^2 - 2.07 \cdot 10^{-26}T^3$$

for 0.5 bar of Ar and

$$\sigma/\text{cm}^2 = 2.80 \cdot 10^{-16} - 1.84 \cdot 10^{-19}T + 4.26 \cdot 10^{-23}T^2 - 2.67 \cdot 10^{-27}T^3$$

for 1 bar of Ar. We tested the calculated cross-sections by following the unimolecular decomposition of HNO<sub>3</sub> and CH<sub>3</sub>OH at temperatures above 1000 K, obtaining agreement within about  $\pm 20\%$ . Similar agreement had been found for measurements with the H<sub>2</sub>/O<sub>2</sub> system in Ref. 11. Alternative expressions for  $\sigma(p, T)$  have recently been used in Ref. 12 based on the oscillator strengths and calculations from Ref. 13, giving

$$\sigma/\text{cm}^2 = 1.77 \cdot 10^{-16} - 6.13 \cdot 10^{-20}T - 4.77 \cdot 10^{-24}T^2 + 3.54 \cdot 10^{-27}T^3$$

for the  $Q_1(4)$  line and  $p=1$  bar. The deviation from our data at 1 bar is 12% at 1050 K and 8% at 2380 K. Like Ref. 12, other authors<sup>14–18</sup> basing their cross section on Ref. 13 estimate the uncertainty of the cross sections to be about 5%. Therefore, we estimate the precision of our HO concentrations to be better than  $\pm 20\%$ .

Reactions mixtures were prepared by passing a flow of Ar through a two-stage saturator filled with nearly 100% H<sub>2</sub>O<sub>2</sub>. The H<sub>2</sub>O<sub>2</sub>/Ar mixtures then were carried through an inlet in the end plate into the shock tube. In order to vary the H<sub>2</sub>O<sub>2</sub> concentration over wider ranges, the H<sub>2</sub>O<sub>2</sub>/Ar stream could be mixed with a pure stream of Ar. Because of substantial adsorption and decomposition of H<sub>2</sub>O<sub>2</sub> at the walls of the shock tube, the initial H<sub>2</sub>O<sub>2</sub> concentration in the shock heated gas mixture was reconstructed from the HO signals: During the first microseconds, the decomposition of H<sub>2</sub>O<sub>2</sub> is dominated by reaction (1). The rate of HO formation during this period, via the well known values of  $k_1$ <sup>4,5</sup> and the HO absorption cross section, led to the initial H<sub>2</sub>O<sub>2</sub> concentration. A determination of the initial H<sub>2</sub>O<sub>2</sub> concentration via the *in situ* uv absorption of H<sub>2</sub>O<sub>2</sub> is by far too insensitive: The weak H<sub>2</sub>O<sub>2</sub> and the much stronger HO<sub>2</sub> uv continua overlap over wide ranges<sup>4,5</sup> and the resulting signals for the here employed low concentrations are too small to be detected with similar sensitivity as HO. Therefore, the recon-

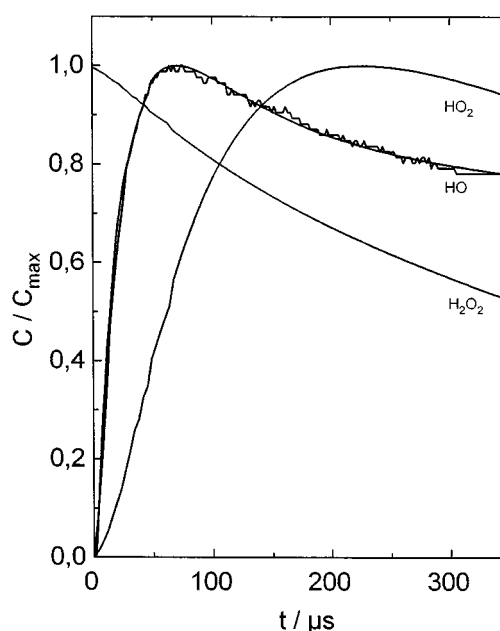


FIG. 1. Calculated concentration-time profiles of H<sub>2</sub>O<sub>2</sub>, HO, and HO<sub>2</sub> in the thermal dissociation of H<sub>2</sub>O<sub>2</sub> ( $c$ =concentration,  $c_{\text{max}}$ =maximum concentration;  $T=1150$  K,  $[\text{Ar}]=5.6 \cdot 10^{-6}$  mol cm<sup>-3</sup>,  $[\text{H}_2\text{O}_2]_{t=0}=6.5 \cdot 10^{-9}$  mol cm<sup>-3</sup>,  $[\text{HO}]_{\text{max}}=2.4 \cdot 10^{-10}$  mol cm<sup>-3</sup>,  $[\text{HO}_2]_{\text{max}}=7.3 \cdot 10^{-10}$  mol cm<sup>-3</sup>; simulated profiles with rate coefficients from Table II, curve with noise: measured HO profile).

struction of initial H<sub>2</sub>O<sub>2</sub> concentrations via HO formation rates provided the by far most reliable access, leaving only the  $\pm 20\%$  uncertainty from the employed absorption cross section.

### III. EVALUATION OF CONCENTRATION-TIME PROFILES

At low initial H<sub>2</sub>O<sub>2</sub> concentrations (1–5 ppm), the unimolecular decomposition of H<sub>2</sub>O<sub>2</sub> could be completely isolated from secondary reactions. With higher relative concentrations of H<sub>2</sub>O<sub>2</sub> (100–1000 ppm in Ar), reactions (2)–(4) then became more important. An orientation about the expected H<sub>2</sub>O<sub>2</sub>, HO, and HO<sub>2</sub> concentration-time profiles was provided by numerical simulation of the mechanism of reactions (1)–(4) using preliminary rate coefficients from Refs. 1 and 2. Whereas  $k_1$  and  $k_4$  have been accurately measured before,<sup>3–7</sup> the values of  $k_2$  and  $k_3$  were fine adjusted in the present work. Using our final set of rate parameters, Fig. 1 presents an example of calculated concentration-time profiles. A comparison of the calculated with a measured HO profile is also given, showing agreement in all details such that no evidence for other processes was present. The HO concentration reaches its maximum after a short time, remaining quasistationary at longer times during which [HO<sub>2</sub>] reaches its maximum. While our earlier conclusions were based on measured H<sub>2</sub>O<sub>2</sub> and HO<sub>2</sub> profiles,<sup>3–7</sup> the present investigations of HO profiles provide a more direct and more accurate access to the values of  $k_2$  and  $k_3$ . We also did modeling including a variety of secondary reactions different from reactions (1)–(4) such as HO+HO→H<sub>2</sub>O+O and other

TABLE I. Experimental conditions and derived rate constants  $k_2$  and  $k_3$ .

$T/$ K	$[Ar]/$ $10^{-6} \text{ mol cm}^{-3}$	$[H_2O_2]/$ $10^{-10} \text{ mol cm}^{-3}$	$k_2/$ $10^{12} \text{ cm}^3 \text{ mol}^{-1} \text{ s}^{-1}$	$k_3/$ $10^{13} \text{ cm}^3 \text{ mol}^{-1} \text{ s}^{-1}$
931	8.2	84	1.6	
978	2.3	22	2.5	
979	2.3	20	2.0	
1012	7.2	53	4.0	
1015	5.1	49	4.0	
1025	2.4	6.5	4.0	
1030	6.7	22	3.2	
1078	2.4	3.6	5.0	
1091	2.4	1.9	5.0	
1110	6.5	33	6.3	
1118	6.2	33	6.3	2.2
1136	5.9	16	7.9	2.0
1152	5.6	65	6.0	1.6
1164	5.3	29	7.0	1.5
1190	5.2	25	7.5	1.3
1226	5.2	21	8.3	1.0
1246	5.1	52	9.0	1.1
1255	5.0	41	9.7	1.0
1278	4.8	34	10	1.1
1296	4.6	29	16	1.2
1362	4.4	11	22	1.6
1384	4.0	6.7	25	1.3
1420	3.9	13	39	2.6
1426	3.8	4.1	27	
1447	3.7	3.5	26	
1455	3.8	3.1	32	
1462	3.9	1.4	100	
1473	3.6	2.3	63	2.5
1481	3.4	3.0	63	
1488	3.5	6.9	130	
1494	3.1	6.1	86	
1502	3.5	2.2	73	2.8
1527	3.4	1.7	130	
1566	3.0	5.7	200	4.9
1678	2.8	1.5	200	

processes with rate parameters from Refs. 1 and 2. The influence of such reactions was always negligible under our conditions.

The numerical analysis of the recorded profiles and the fit of  $k_2$  and  $k_3$  is straight forward. However, a simplified analysis is already obtainable in the following way which shows that the analysis of HO concentration profiles allows for a nearly independent determination of the values of  $k_2$  and  $k_3$ : With reactions (1)–(4), the maximum concentrations of HO are given by

$$[HO]_{\max} = \frac{2k_1[Ar]}{k_2 + k_3[HO_2]/[H_2O_2]}. \quad (5)$$

The concentrations of HO<sub>2</sub> at times, when the HO maximum is reached, are generally still so low that  $k_2 \gg k_3[HO_2]/[H_2O_2]$  in Eq. (5) and hence

$$k_2 \approx 2k_1[Ar]/[HO]_{\max}. \quad (6)$$

After having reached quasistationary state and passed through its maximum, [HO] decreases while [HO<sub>2</sub>] still increases until it passes through a maximum. First estimations of  $k_2$ , therefore, were obtained from Eq. (6) while  $k_3$  was derived from the later HO decay such as given by Eq. (5).

Not much fine tuning of  $k_2$  and  $k_3$  was required to arrive at perfect agreement with the full HO profiles. This is, e.g., demonstrated in Fig. 1.

Table I summarizes conditions and derived values of the rate constants  $k_2$  and  $k_3$  for a selected set of our experiments (the values for  $k_1$  and  $k_4$  used in the analysis are given in the next section). Following the simplified analysis leading to Eqs. (5) and (6), one easily realizes that the accuracy of the derived values of  $k_2$  neither depended on noise of the measured HO signals nor on the fitting procedure but on the ratio of  $k_1/[HO]_{\max}$ ; see Eq. (6). The uncertainty of  $k_2$ , hence, was that of the ratio  $k_1/\sigma(\text{HO})$ . On the basis of the separate determinations of  $k_1$  ( $\Delta k_1/k_1 = 25\%$ )<sup>4,5</sup> and  $\sigma(\text{HO})$  [ $\Delta\sigma(\text{HO})/\sigma(\text{HO}) = 20\%$ ] from Refs. 9 and 10, we estimate this ratio to be accurate within  $\pm 40\%$ . The decay of [HO] after reaching the maximum is mainly determined by the ratio  $k_2/k_3$ . One may demonstrate the sensitivity of the observed [HO] profiles on the individual values of  $k_2$  and  $k_2/k_3$  (leaving  $k_1$ ,  $k_4$ ,  $[H_2O_2]_{t=0}$ , and  $\sigma(\text{HO})$  fixed). Figures 2 and 3 show concentration–time profiles for typical low and high temperature conditions used in our work. The simulation was done with optimum values of  $k_2$  and  $k_2/k_3$  and variations of  $\pm 40\%$  of  $k_2$  and a factor of 2 in the ratio  $k_2/k_3$ . The figures

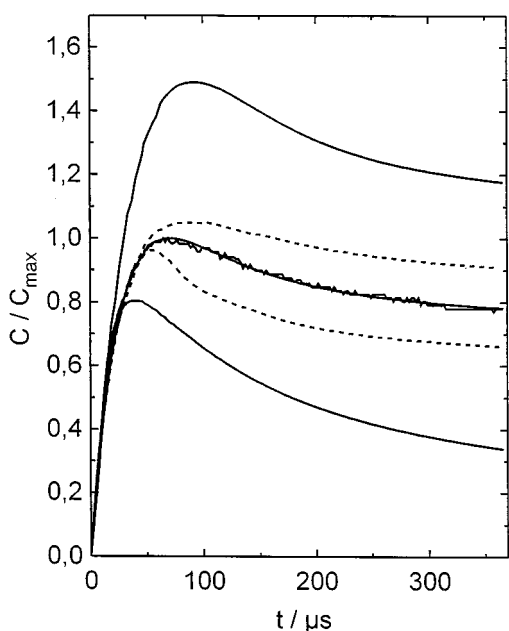


FIG. 2. Sensitivity of calculated concentration-time profiles of HO at 1150 K on  $k_2$  and  $k_2/k_3$  (full lines:  $k_2+40\%$  (lower curve),  $k_2-40\%$  (upper curve); dashed lines:  $k_2/k_3 \cdot 2$  (upper curve),  $k_2/k_3 \cdot 0.5$  (lower curve); line with noise: measured HO profile).

well illustrate that the fitting is more certain in  $k_2$  than the basic uncertainty of  $\pm 40\%$  of the ratio  $k_1/\sigma$  (HO). At the same time, the fitting of  $k_2/k_3$  and, hence, of  $k_3$  is more certain than a factor of 2.

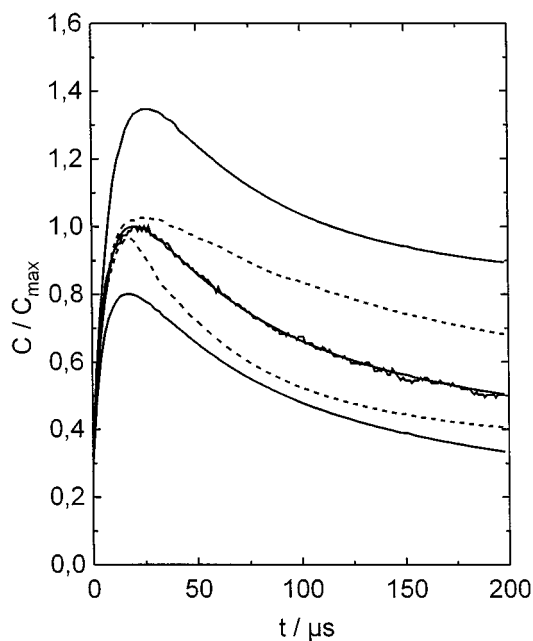


FIG. 3. Sensitivity of calculated concentration-time profiles of HO at 1566 K on  $k_2$  and  $k_2/k_3$  (full lines:  $k_2+40\%$  (lower curve),  $k_2-40\%$  (upper curve); dashed lines:  $k_2/k_3 \cdot 2$  (upper curve),  $k_2/k_3 \cdot 0.5$  (lower curve); line with noise: measured HO profile).

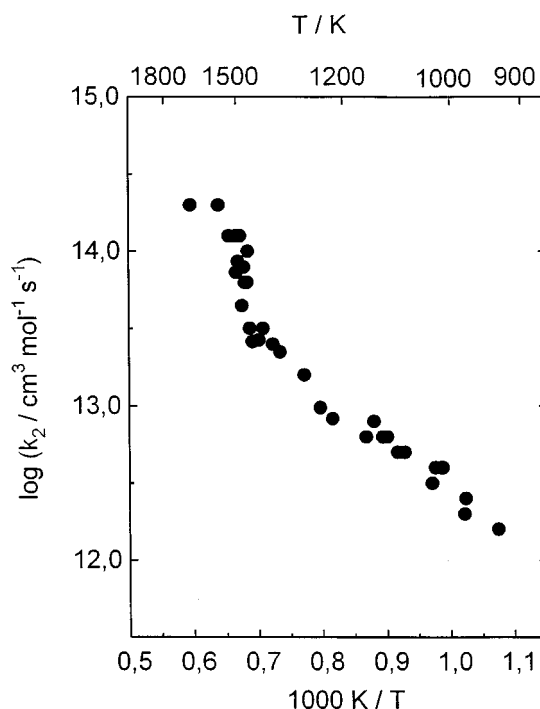


FIG. 4. Rate constants for the reaction  $\text{HO} + \text{H}_2\text{O}_2 \rightarrow \text{H}_2\text{O} + \text{HO}_2$ .

## IV. RESULTS AND DISCUSSION

### A. Results for the reaction $\text{HO} + \text{H}_2\text{O}_2 \rightarrow \text{HO}_2 + \text{H}_2\text{O}$

Figure 4 shows an Arrhenius representation of our results for  $k_2$ . With increasing temperature, one observes a steepening of the Arrhenius plot before the increase of  $k_2$  levels off at the highest temperatures where  $k_2$  exceeds  $10^{14} \text{ cm}^3 \text{ mol}^{-1} \text{ s}^{-1}$ . The non-Arrhenius character of the rate constant becomes even more apparent when literature values<sup>19–24</sup> from lower temperatures are included, see Fig. 5. At low temperatures, reaction (2) has a small positive activation energy which changes to a much larger positive activation energy before a leveling off sets in. The marked change of the activation energy near 800 K, which we earlier derived from the analysis of HO<sub>2</sub> yields in the H<sub>2</sub>O<sub>2</sub> decomposition,<sup>3</sup> is completely confirmed by the present analysis of HO profiles. Apart from the high temperature leveling off, the results can well be represented by the sum of two Arrhenius expressions

$$k_2 = [1.7 \cdot 10^{18} \exp(-14\,800 \text{ K}/T) + 2.0 \cdot 10^{12} \times \exp(-215 \text{ K}/T)] \text{ cm}^3 \text{ mol}^{-1} \text{ s}^{-1} \quad (7)$$

for  $240 \leq T \leq 1600 \text{ K}$ .

For  $T \geq 1600 \text{ K}$ , apparently a value of  $k_2 \approx 2.0 \cdot 10^{14} \text{ cm}^3 \text{ mol}^{-1} \text{ s}^{-1}$  is approached. Figure 5 includes the representation from Eq. (7).

One may ask for an interpretation of so strongly non-Arrhenius temperature dependences of rate constants as shown for  $k_2$  in Fig. 5. One possible explanation could be the formation of intermediate complexes such that the overall rate of the “elementary reaction” is given by the rate of

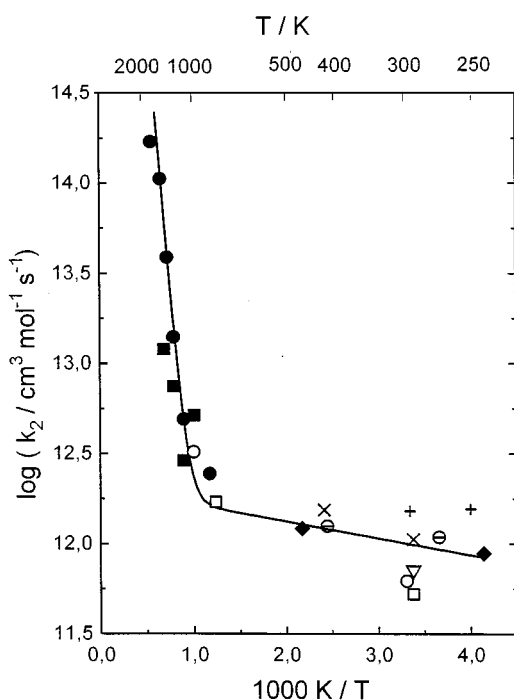


FIG. 5. Rate constants for the reaction  $\text{HO}+\text{H}_2\text{O}_2\rightarrow\text{H}_2\text{O}+\text{HO}_2$  (experiments in Ar at 400–600 mbar, this work:  $\bullet$ , full line from Eq. (7); measurements at 10–1000 mbar from Ref. 19:  $\square$ , Ref. 20:  $\blacklozenge$ , Ref. 21:  $\circ$ , Ref. 22:  $\times$  and  $\ominus$ , Refs. 3, 7:  $\blacksquare$ , Ref. 23:  $+$ , Ref. 24:  $\nabla$ ).

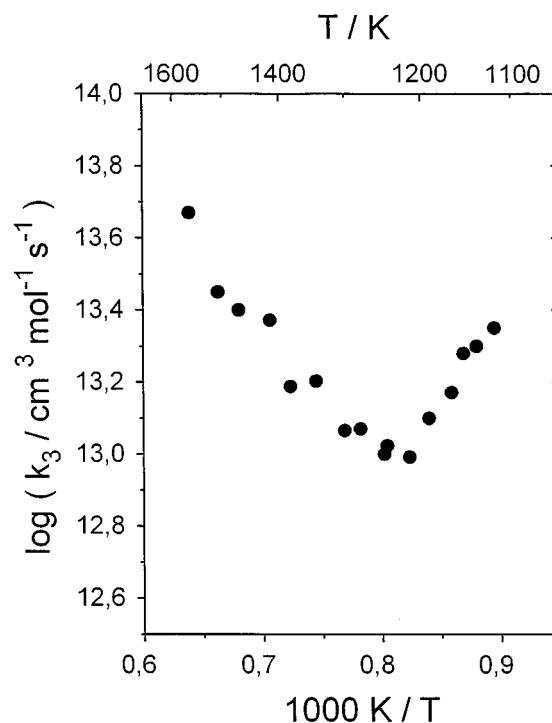


FIG. 7. Rate constants for the reaction  $\text{HO}+\text{HO}_2\rightarrow\text{H}_2\text{O}+\text{O}_2$ .

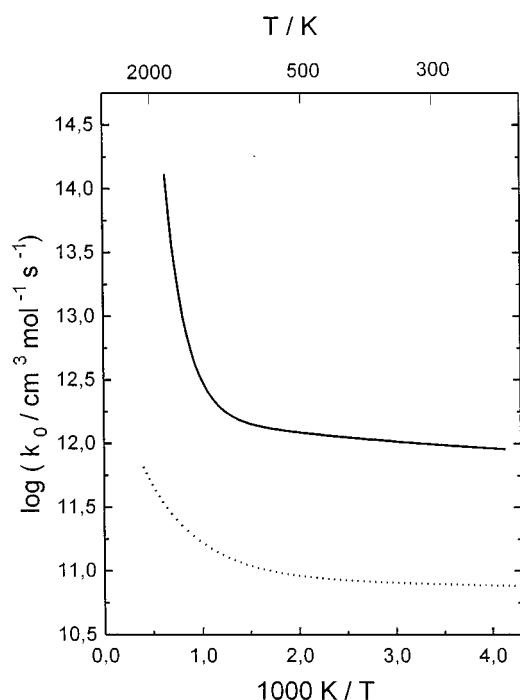


FIG. 6. Comparison of rate constants for the reaction  $\text{HO}+\text{H}_2\text{O}_2\rightarrow\text{H}_2\text{O}+\text{HO}_2$  (full line) with the reaction  $\text{HO}+\text{CO}\rightarrow\text{H}+\text{CO}_2$  (dashed line).

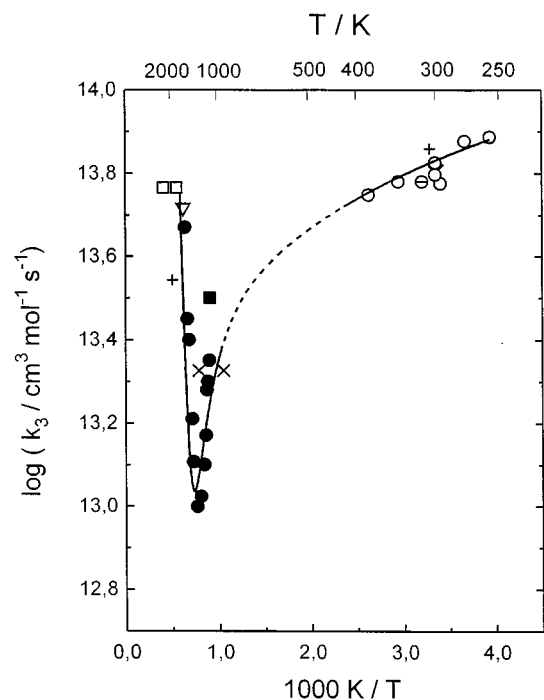


FIG. 8. Rate constants for the reaction  $\text{HO}+\text{HO}_2\rightarrow\text{H}_2\text{O}+\text{O}_2$  (this work:  $\bullet$ , full lines: measured high and low temperature dependence, dashed line: possible temperature dependence, measurements from Ref. 26:  $\nabla$ , Ref. 27:  $\ominus$ , Ref. 28:  $\blacklozenge$ , Ref. 29:  $\square$ , Ref. 30:  $\blacksquare$ , Ref. 31:  $+$ , Ref. 3:  $\times$ ).

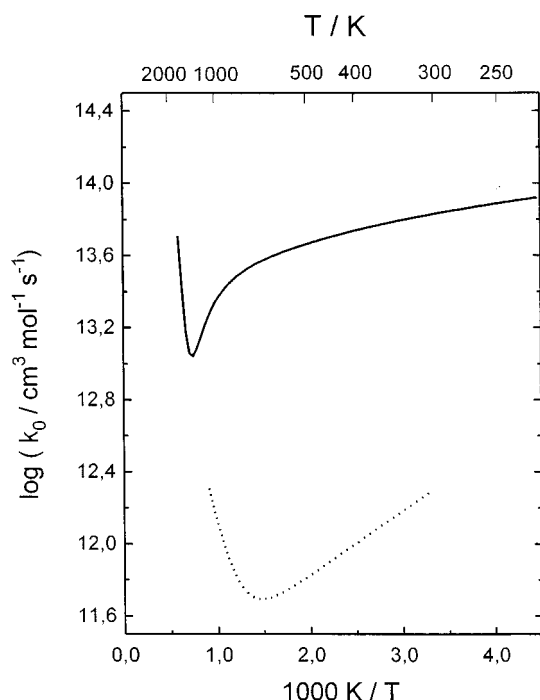


FIG. 9. Comparison of rate constants for the reaction  $\text{HO} + \text{HO}_2 \rightarrow \text{H}_2\text{O} + \text{O}_2$  (full line, see Fig. 8) with the reaction  $\text{HO}_2 + \text{HO}_2 \rightarrow \text{H}_2\text{O}_2 + \text{O}_2$  (dashed line).

formation of the complex and the subsequent competition between forward and backward dissociations. It was shown in Ref. 8 that a multitude of possible temperature dependences arises in this class of reactions, apparent activation energies and preexponential factors not being related to barrier heights and gas kinetic collision frequencies in a simple way. Besides anomalous temperature dependences, this class of reactions sometimes also reveals its very nature by pressure dependences of the apparent second-order rate constants. However, the latter effect is only observed when the dissociation rates of the complex become smaller than the collisional stabilization rates. A particularly complete picture of this type of behavior recently was observed<sup>25</sup> for the reaction



which involves the well known HOCO intermediate. In Fig. 6 we compare the limiting low pressure rate constant  $k_{8,0}$  of this reaction with  $k_2$ . The temperature dependences of the two reactions are of similar strongly non-Arrhenius character. One, therefore, may speculate whether reaction (2) also

involves intermediate complex formation. In this case, however, the intermediate  $\text{H}_3\text{O}_3$  species has not yet been well characterized. A pressure dependence has also not been observed as yet. However, this would just indicate that the dissociation rate of excited  $\text{H}_3\text{O}_3^*$  with the applied pressures below a few bar was not matched by a collisional stabilization rate, i.e., the well depth of the complex would have to be considerably smaller than the  $130 \text{ kJ mol}^{-1}$  derived for HOCO.<sup>25</sup> Experiments at higher pressures and lower temperatures or direct trapping of the intermediate would provide the proof. As long as this is not available, at least we take the similarity of the non-Arrhenius temperature dependence of  $k_2$  and  $k_{8,0}$  as strong evidence for the implication of  $\text{H}_3\text{O}_3$  intermediate complex formation.

## B. Results for the reaction $\text{HO} + \text{HO}_2 \rightarrow \text{H}_2\text{O} + \text{O}_2$

The temperature dependence of  $k_3$  is weaker than that of  $k_2$  and it is characteristically different. Figure 7 shows our results. There is a rate constant minimum near 1250 K which is located at higher temperatures than that for reaction (4) which was found near to 800 K.<sup>7</sup> The rate constant  $k_3$  decreases from a value of  $2.0 \cdot 10^{13}$  at 1100 K to a minimum value of  $1.1 \cdot 10^{13}$  at 1250 K, and rises again to a value of  $4.5 \cdot 10^{13} \text{ cm}^3 \text{ mol}^{-1} \text{ s}^{-1}$  at 1600 K. Again a non-Arrhenius temperature dependence is observed, in particular when our high temperature results are compared with literature data<sup>26–31</sup> for lower temperatures; see Fig. 8. The initially observed pressure dependence near room temperature apparently was an artifact, see Ref. 30.

In Fig. 9 we compare the temperature dependences of the low pressure rate constants  $k_{4,0}$  and  $k_{3,0}$ . For reactions (3) and (4) one observes rate constant minima which, however, are developed to different extent. Furthermore, for reaction (4) a pressure dependence of  $k_4$  was observed near room temperature<sup>32,33</sup> which apparently was not present below 1 bar in reaction (3). If one again attributes the pressure and non-Arrhenius temperature dependence of  $k_4$  to a reaction involving an  $\text{H}_2\text{O}_4$  intermediate complex, one is tempted to draw similar conclusions on reaction (3), i.e., to postulate an  $\text{H}_2\text{O}_3$  intermediate complex. The absence of a pressure effect below 1 bar for reaction (3) at 300 K then again has to be attributed to a shorter lifetime of excited  $\text{H}_2\text{O}_3^*$  in comparison to excited  $\text{H}_2\text{O}_4^*$ .

The conclusions on a mechanism involving intermediate complex formation in reactions (2)–(4) are still tentative. They are based on anomalous temperature dependences and,

TABLE II. Summary of rate constants for reactions (1)–(4).

Reaction	$T$ (K)	$k$ ( $\text{cm}^3 \text{ mol}^{-1} \text{ s}^{-1}$ )	Reference
(1) $\text{H}_2\text{O}_2 + \text{Ar} \rightarrow 2\text{HO} + \text{Ar}$	950–1450	$k_1 = [\text{Ar}] \cdot 5.8 \cdot 10^{31} \cdot T^{-4.55} \exp(-25580 \text{ K}/T)$	4, 5, This work
(2) $\text{HO} + \text{H}_2\text{O}_2 \rightarrow \text{H}_2\text{O} + \text{HO}_2$	240–1700	$k_2 = 1.7 \cdot 10^{18} \exp(-14800 \text{ K}/T) + 2.0 \cdot 10^{12} \exp(-215 \text{ K}/T)$	This work
(3) $\text{HO} + \text{HO}_2 \rightarrow \text{H}_2\text{O} + \text{O}_2$	1100–1600	see Fig. 7	This work
(4) $\text{HO}_2 + \text{HO}_2 \rightarrow \text{H}_2\text{O}_2 + \text{O}_2$	300–1100	$k_4 = 4.2 \cdot 10^{14} \exp(-6030 \text{ K}/T) + 1.3 \cdot 10^1 \exp(820 \text{ K}/T)$	7

in part, the observation of pressure dependences. Therefore, more experiments extending into the high pressure range, such as performed for the HO+CO reaction,<sup>25</sup> are desirable. Also trapping of H<sub>3</sub>O<sub>3</sub>, H<sub>2</sub>O<sub>3</sub>, and H<sub>2</sub>O<sub>4</sub> species would be helpful. Nevertheless, a final proof can only be obtained by combining extensive measurements of the described type with *ab initio* calculations of the complete potential energy surface of the reaction. The HO+CO reaction serves as a model system for this purpose.

We finally summarize all rate constants of reaction (1)–(4) such as measured and combined with low temperature data in the present work (see Table II). Apart from determining  $k_2$  and  $k_3$ , we also reevaluated  $k_1$  from earlier experiments of Refs. 4 and 5 using the new set of rate data for reactions (2)–(4). As this led to only a minor correction of  $k_1$  we do not discuss this reevaluation here.

## ACKNOWLEDGMENTS

We thank Dr. M. Röhrig for technical assistance with the ring laser system. Financial support of this work by the Deutsche Forschungsgemeinschaft (SFB 357 “Molekulare Mechanismen unimolekularer Prozesse”) is gratefully acknowledged.

- <sup>1</sup>R. Atkinson, D. L. Baulch, R. A. Cox, R. F. Hampson, J. A. Kerr, and J. Troe, *J. Phys. Chem. Ref. Data* **21**, 1125 (1992).
- <sup>2</sup>D. L. Baulch, C. J. Cobos, R. A. Cox, P. Frank, Th. Just, J. A. Kerr, M. J. Pilling, J. Troe, R. W. Walker, and J. Warnatz, *J. Phys. Chem. Ref. Data* **92**, 411 (1992).
- <sup>3</sup>H. Hippler and J. Troe, *Chem. Phys. Lett.* **192**, 333 (1992).
- <sup>4</sup>J. Troe, *Ber. Bunsenges. Phys. Chem.* **73**, 946 (1969).
- <sup>5</sup>H. Kijewski and J. Troe, *Helvetica Chim. Acta* **55**, 205 (1972).
- <sup>6</sup>H. Kijewski and J. Troe, *Int. J. Chem. Kin.* **3**, 223 (1971).
- <sup>7</sup>H. Hippler, J. Troe, and J. Willner, *J. Chem. Phys.* **93**, 755 (1990).
- <sup>8</sup>J. Troe, *J. Chem. Soc. Faraday Trans.* **90**, 2303 (1994).
- <sup>9</sup>G. H. Dieke and H. M. Crosswhite, *J. Quant. Spectrosc. Radiat. Transfer* **2**, 97 (1962).
- <sup>10</sup>D. R. Crosley and R. K. Lengel, *J. Quant. Spectrosc. Radiat. Transfer* **15**, 579 (1975).
- <sup>11</sup>M. Braun-Unkhoff, C. Naumann, K. Wintergerst, and P. Frank, *VDI Berichte 1090*, 16. Deutscher Flammentag (VDI, Düsseldorf, 1993), p. 287.
- <sup>12</sup>M. S. Wooldridge, R. K. Hanson, and C. T. Bowman, *Int. J. Chem. Kin.* **26**, 389 (1994).
- <sup>13</sup>A. Goldman and J. R. Gillis, *J. Quant. Spectrosc. Radiat. Transfer* **25**, 111 (1981).
- <sup>14</sup>R. K. Hanson, S. Siamak, G. Kychakoff, and A. R. Booman, *Appl. Opt.* **22**, 641 (1983).
- <sup>15</sup>D. A. Masten, R. K. Hanson, and C. T. Bowman, *J. Phys. Chem.* **94**, 7119 (1990).
- <sup>16</sup>H. Du and J. P. Hessler, *J. Phys. Chem.* **96**, 1077 (1992).
- <sup>17</sup>W. A. von Drasek, S. Okajima, J. H. Kiefer, P. J. Ogren, and J. P. Hessler, *Appl. Opt.* **29**, 4899 (1990).
- <sup>18</sup>T. Yuan, C. Wang, C.-L. Yu, and M. Frenklach, *J. Phys. Chem.* **95**, 1258 (1991).
- <sup>19</sup>R. F. Baldwin and R. W. Walker, *J. Chem. Soc. Faraday Trans.* **75**, 140 (1979).
- <sup>20</sup>U. C. Sridharan, B. Reimann, and F. Kaufman, *J. Chem. Phys.* **73**, 1286 (1980).
- <sup>21</sup>P. H. Wine, D. H. Semmes, and A. R. Ravishankara, *J. Chem. Phys.* **75**, 4390 (1981).
- <sup>22</sup>G. L. Vaghjiani and A. R. Ravishankara, *J. Phys. Chem.* **93**, 7833 (1989).
- <sup>23</sup>E. R. Lovejoy, T. P. Murrells, A. R. Ravishankara, and C. J. Howard, *J. Phys. Chem.* **94**, 2386 (1990).
- <sup>24</sup>A. A. Turnipseed, G. L. Vaghjiani, T. Gierczak, J. E. Thompson, and A. R. Ravishankara, *J. Chem. Phys.* **95**, 3244 (1991).
- <sup>25</sup>D. Fulle, H. Hamann, H. Hippler, and J. Troe, *J. Chem. Phys.* (in press, 1995).
- <sup>26</sup>J. Peeters and G. Mahnen, *14th Symp. (Int.) on Combust.* (The Combustion Institute, Pittsburgh, 1973), p. 133.
- <sup>27</sup>J. P. Burrows, R. A. Cox, and R. G. Derwent, *J. Photochem.* **16**, 147 (1981).
- <sup>28</sup>R.-R. Lii, R. A. Gorse, M. C. Sauer, and S. Gordon, *J. Phys. Chem.* **84**, 819 (1980).
- <sup>29</sup>J. M. Goodings and A. N. Hayhurst, *J. Chem. Soc. Faraday Trans. 2* **84**, 745 (1988).
- <sup>30</sup>L. F. Keyser, *J. Phys. Chem.* **92**, 1193 (1988).
- <sup>31</sup>W. B. DeMore, *J. Phys. Chem.* **86**, 121 (1982).
- <sup>32</sup>P. D. Lightfoot, B. Veyret, and R. Lesclaux, *Chem. Phys. Lett.* **150**, 120 (1988).
- <sup>33</sup>M. J. Kurylo, P. A. Oulette, and A. H. Laufer, *J. Phys. Chem.* **90**, 437 (1986).